Journal of Power Sources 184 (2008) 197–203

Contents lists available at ScienceDirect

Journal of Power Sources

journal homepage: www.elsevier.com/locate/jpowsour

Fabrication and investigation of SiO_2 supported sulfated zirconia/Nafion® self-humidifying membrane for proton exchange membrane fuel cell applications

Cheng Bi [a,b], Huamin Zhang [a,*], Yu Zhang [a,b], Xiaobing Zhu [c,d], Yuanwei Ma [a,b], Hua Dai [a,b], Shaohua Xiao [a,b]

[a] *Proton Exchange Membrane Fuel Cell Key Materials and Technology Laboratory, Dalian Institute of Chemical Physics, Chinese Academy of Sciences, 457 Zhongshan Road, Dalian 116023, China*
[b] *Graduate University of Chinese Academy of Sciences, Beijing 100039, China*
[c] *Center for Innovative Fuel Cell and Battery Technologies, School of Materials Science and Engineering, Georgia Institute of Technology, 771 Ferst Drive NW, Atlanta, GA 30332-0245, USA*
[d] *Department of Chemical & Biomolecular Engineering, University of Houston, 4800 Calhoun Avenue, S166 Engineering Building 1, Houston, TX 77204-4004, USA*

ARTICLE INFO

Article history:
Received 11 April 2008
Received in revised form 2 June 2008
Accepted 5 June 2008
Available online 20 June 2008

Keywords:
Proton exchange membrane fuel cell
Self-humidifying membrane
Nafion®
Silicon oxide supported sulfated zirconia
Proton conductivity

ABSTRACT

A self-humidifying composite membrane based on Nafion® hybrid with SiO_2 supported sulfated zirconia particles (SiO_2–SZ) was fabricated and investigated for fuel cell applications. The bi-functional SiO_2–SZ particles, possessing hygroscopic property and high proton conductivity, were homemade and as the additive incorporated into our composite membrane. X-ray diffraction (XRD) and Fourier infrared spectrum (FT-IR) techniques were employed to characterize the structure of SiO_2–SZ particles. Scanning electronic microscopy (SEM) and energy dispersive spectroscopy (EDS) measurements were conducted to study the morphology of composite membrane. To verify the advantages of Nafion®/SiO_2–SZ composite membrane, the IEC value, water uptake, proton conductivity, single cell performance and areal resistance were compared with Nafion®/SiO_2 membrane and recast Nafion® membrane. The single cell employing our Nafion®/SiO_2–SZ membrane exhibited the highest peak power density of 0.98 W cm^{-2} under dry operation condition in comparison with 0.74 W cm^{-2} of Nafion®/SiO_2 membrane and 0.64 W cm^{-2} of recast Nafion® membrane, respectively. The improved performance was attributed to the introduction of SiO_2–SZ particles, whose high proton conductivity and good water adsorbing/retaining function under dry operation condition, could facilitate proton transfer and water balance in the membrane.

1. Introduction

In the past decades, proton exchange membrane fuel cells (PEMFCs) attracted much more attention due to their advantages of high power density, simplicity of operation, high-energy conversion efficiency and near zero harmful emissions [1–3]. Three potential applications, such as automotive, stationary and portable power sources, highly motivate current R&D of PEMFCs [4]. In general, PEMFCs are operated with humidified fuel and oxidant at around 80 °C [5]. The operation conditions require fuel and oxidant are firstly fed into the humidifying subsystem prior to entry into the cell. However, the external humidifying equipment makes the system more complex and increases its weight, volume and cost, which burdens fuel cell stack design. Obviously, the promoted operation of PEMFCs without external humidifying subsystem seems more attractive and valuable.

As a standard membrane material, Nafion®-a poly(perfluorosulfonic acid) membrane (product of DuPont), is widely applied for PEMFCs. But when it is operated under low humidity condition, the proton conductivity will decrease with reduced water content due to the shrinkage of the hydrated ionic clusters [6–12]. To enhance the water retention of Nafion® and related membranes under low humidity conditions, many previous works focused on incorporating some hygroscopic oxide particles into membrane matrix [13–15]. Adjemian et al. [14] reported that the composite membrane with silicon oxide as the additive had lower resistance under reduced relative humidity (RH) in an operating PEMFC. Watanabe et al. [15] also investigated a series of Nafion® composite membranes incorporated with hygroscopic oxides (such as SiO_2, TiO_2) in H_2/O_2 PEMFCs with low external humidification. Their results indicated that Nafion®/SiO_2 composite membrane showed the best performance due to the highest water sorption qualities

* Corresponding author. Tel.: +86 411 84379072; fax: +86 411 84665057.
E-mail address: zhanghm@dicp.ac.cn (H. Zhang).

0378-7753/$ – see front matter.
doi:10.1016/j.jpowsour.2008.06.019

of SiO_2 among the above mentioned oxides. However, this hygroscopic property could not always lead to a desired performance improvement under fully humidified condition. Most researchers thought that the proton conductivity of the composite membranes under fully humidified condition was remarkably reduced due to incorporating with these non-proton-conductive hygroscopic oxides [16–20].

To minimize the loss of proton conductivity caused by adding the silicon oxide particles, many efforts have been made. Rhee et al. [21] and Munakata et al. [22] grafted the organic sulfonic acid group onto the surface of silicon oxide by reacting with 3-mercaptopropyltrimethoxysilane (SH oxidation). Unfortunately, the sulfonic acid group attached to the aliphatic propylsilane chain suffered from poor thermal stability [21]. Another approach had been attempted by Shao et al. [23]. The Nafion® composite membranes, which incorporated with phosphotungstic acid (PWA)/silicon oxide particles, showed higher proton conductivity at low RH than pristine Nafion® membrane. But the issue of PWA tending to dissolve in the hydrated membrane raises a major concern in the operating PEMFCs.

Sulfated zirconia (SO_4^{2-}/ZrO_2, SZ) is considered as the strongest solid acid among all known solids (Hammett acid strength $H_0 = -16.03$) [24]. In our previous work, owing to its high proton conductivity, we had applied it as an additive to fabricate composite membranes for PEMFCs operated under low RH condition [25–27]. In recent years, to improve textural properties and enhance thermal stability of the SZ, much attention has been paid to prepare oxides supported SZ such as SiO_2–SZ [28–31]. Until now, there is no application of SiO_2 supported SZ as an additive in self-humidifying composite membranes for PEMFCs applications.

In this paper, we presented Nafion® hybrid with SiO_2–SZ (Nafion®/SiO_2–SZ) self-humidifying composite membrane to improve the single cell performance under both wet and dry conditions. As displayed in Fig. 1, the SiO_2–SZ particles in the polymer matrix can not only adsorb water due to the hygroscopic property of silicon oxide support, but also transfer proton due to the acidic property of SZ. So it is expected to effectively minimize the loss of proton conductivity caused by introducing the silicon oxide particles and improve the composite membrane conductivity under various operation conditions. The structure of the SiO_2–SZ particles and the self-humidifying membrane were characterized by X-ray diffraction (XRD), Fourier infrared spectrum (FT-IR), scanning electron microscopy (SEM), and energy dispersive spectroscopy (EDS). To understand the promoted self-humidification effect by adding the SiO_2–SZ particles, the physicochemical and electrochemical properties of the Nafion®/SiO_2–SZ and Nafion®/SiO_2 self-humidifying membranes were compared, such as IEC, water uptakes, and proton conductivity. The single cell performances and the areal resistances of the two self-humidifying composite membranes and recast Nafion® membrane were also investigated under wet and dry conditions.

2. Experimental

2.1. Preparation of the SiO_2–SZ particles and self-humidifying membranes

The silicon oxide supported sulfated zirconia particles was prepared by impregnation of commercial silicon oxide support (BET surface area of 112 $m^2\,g^{-1}$, average particle size of 20 nm, made in Japan) with $ZrO(NO_3)_2$ in 0.5 M sulfuric acid solution and drying at 80 °C overnight, followed by calcining in air at 600 °C for 2 h. The SZ loading on the silicon oxide support is about 27.4 wt.%.

The Nafion®/SiO_2–SZ membrane was prepared by solution-cast method. The pure Nafion® resin was firstly obtained by evaporation of 5 wt.% Nafion® solution (Dupont Fluoroproducts, EW = 1100 g mol^{-1} SO_3H) at 100 °C under vacuum for 24 h until dry, then redissolved in a solvent containing *N*,*N*-dimethylformamide (DMF) at 60 °C in a closed vessel to obtain 5 wt.% modified Nafion® solution. The 3 wt.% SiO_2–SZ particles (by weight of dry Nafion®) was added to 5 wt.% modified Nafion® solution and stirred with a magnetic stirrer for at least 4 h to form a homogenous solution. The resulting solution was cast onto a clean flat glass and then removed at 60 °C for 12 h followed by further drying at 130 °C under a vacuum. Finally, the membrane was purified by heating at 80 °C in the solution of 3 wt.% H_2O_2, de-ionized water, 0.5 M H_2SO_4 and de-ionized water for 2 h, respectively. For comparison, the Nafion®/SiO_2 and recast Nafion® membranes were prepared in the same way. The thickness values of the membranes were about ca. 50 μm, which was determined by electronic outside micrometers (resolution, 0.001 mm; Qinghai Measuring & Cutting Tools Co. Ltd., China).

2.2. Characterizations of the membranes

2.2.1. XRD analysis of the SiO_2–SZ particles

To gather information of the SiO_2–SZ particles, the X-ray powder diffraction (XRD) analysis was performed using a Panalytical X'pert PRO diffractometer (Philps X'pert PRO) with Cu Kα radiation source. The X-ray diffractogram was obtained for 2θ varying between 10° and 85°.

2.2.2. FT-IR spectrum analysis

FT-IR spectrum of the SiO_2–SZ and SiO_2 were recorded on a JASCO FT-IR 4100 spectrometer to further verify the structure of SiO_2–SZ particles. FT-IR spectrum was measured for the pellets with

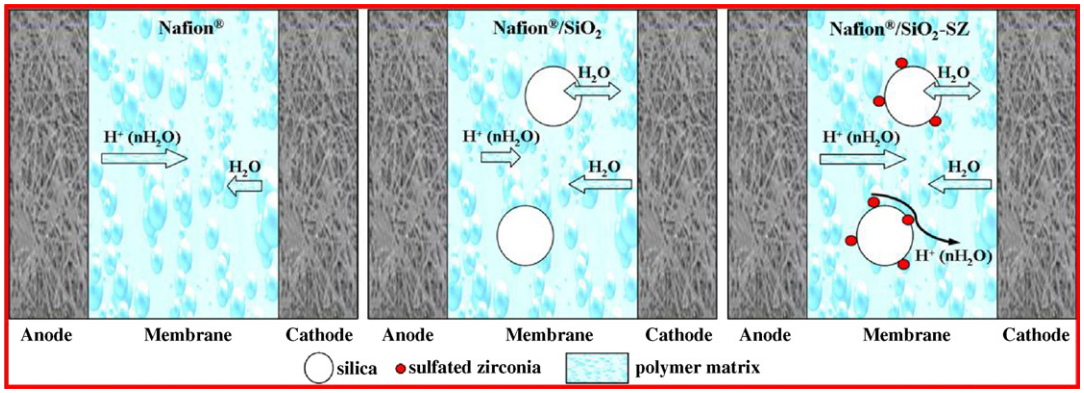

Fig. 1. Schematic diagram of the Nafion®, Nafion®/SiO_2 and Nafion®/SiO_2–SZ self-humidifying membrane.

KBr without special thermal treatment in the absorbance mode with resolution of 2 cm^{-1}.

2.2.3. SEM–EDS analysis of self-humidifying membrane

The cross-sectional morphology of the Nafion®/SiO_2–SZ composite membrane was investigated by SEM (JEOL 6360LV, Japan). The distributions of silicon, zirconium, sulfur and fluorine elements along the membrane cross-section were detected by EDS technique (Oxford Instruments Microanalysis 1350).

2.2.4. Ion exchange capacity (IEC) measurement

The IEC values of membranes were determined by titration as follows [32]: 1–2 g of the samples were placed in 0.5 M aqueous NaOH and kept still for 1 day. The solution was then back titrated with 0.1 M HCl using phenolphthalein as an indicator.

2.2.5. Water uptakes of the membranes

The membrane samples were pretreated by the following procedure: boiling in 3 wt.% hydrogen peroxide, rinsing in boiling water, boiling in 0.5 M sulfuric acid, and finally rinsing in boiling water (1 h for each step) [11]. To determine total water content, the above-pretreated membranes were removed from liquid water, blotted dry to remove the excess surface water, and quickly weighed in a closed vessel. The membrane samples were dried at 105 °C for 10 h under vacuum, and the total water content was determined from the difference between wet and dry weights [11]. For measurement of the bound water content, the above-pretreated samples were heated in a high resolution thermo-gravimetric analyzer (TGA, PerkinElmer Instruments) at a rate of 10 °C min^{-1} from 30 to 200 °C with nitrogen as carrier gas. The weight loss percentage of the membranes in the temperature ranging from 100 to 150 °C, which indicates the bound water content, was recorded [33]. The bound water content was obtained by subtracting the dry weight at 150 °C from the wet weight at 100 °C.

The total water content and bound water content of the membranes is calculated according to the following equations:

$$\Delta W\,(\%) = \frac{W_{\text{wet}} - W_{\text{dry}}}{W_{\text{dry}}} \times 100 \tag{1}$$

$$\lambda_{(H_2O/SO_3H)} = \frac{W_{\text{wet}} - W_{\text{dry}}}{18 W_{\text{dry}}} \times \text{EW} \tag{2}$$

where W_{wet} and W_{dry} represent the weight of the wet and dry membrane, respectively. ΔW and λ parameters represent the mass content of water uptake and water molecule number per $-SO_3H$ group of the membranes, respectively. Subtraction of the bound water content from the total water content gives the bulk water content.

2.2.6. Proton conductivity measurement of the membranes by EIS

The EIS technique was utilized to measure membrane resistance. The results obtained in the form of resistance are based on the geometric area and membrane thickness and then reported as conductivity [34]. The ac impedance spectroscopy measurements were carried out using a frequency response detector (EG&G Model 1025) combined with a potentiostat/galvanostat (EG&G Model 273A). The membrane resistance was measured by impedance spectroscopy in the frequency range of 100 MHz to 100 kHz. The gas flow of H_2/O_2 was fixed at 80/100 ml min^{-1}, respectively [34]. The operating temperature of the cell was maintained to 60 °C. Two different RH operation modes were designed according to R_f. [35]. One mode was RH = 100%, which represented fully humidified H_2 and O_2 was fed into the cell; the other mode was RH = 0%, which represented dry H_2 and O_2 were fed into the cell. After the operation mode was chosen, the cell was put at the 500 mA cm^{-2} for 10 h until obtaining the stable cell voltage value. Then the cell was put under open circuit potential condition with the H_2 and O_2 pipelines dead end for 20 min (to avoid the membrane being blow-dried by hot flowing gas). After that, the resistance value was measured [35]. At last, the proton conductivity was calculated according to the following equation:

$$\sigma = \frac{d}{RA} \tag{3}$$

where σ represents the proton conductivity of membranes, d represents the thickness of membranes, R and A represent the membrane resistance and the active area of MEAs, respectively.

2.2.7. Single PEM fuel cell tests

The membrane electrode assemblies (MEAs) were fabricated by hot-pressing the anode and the cathode to the membrane at 140 °C and 10 MPa for 2 min. The Pt loading in the anode and the cathode were 0.3 and 0.5 mg cm^{-2}, respectively. The Nafion® loading in both the anode and the cathode were 0.4 mg cm^{-2}. The active area of MEAs was 5 cm^2. The MEA was placed in a single cell using stainless steel as the end plates and stainless mesh as the current collectors.

To check the self-humidifying effect of the Nafion®/SiO_2–SZ and Nafion®/SiO_2 composite membrane, the single cell was kept running with dry H_2 and O_2. After stable cell performance was maintained for 8 h, the cell voltages at different current densities were recorded. The single cells with the Nafion®/SiO_2–SZ and Nafion®/SiO_2 membrane were evaluated at 60 °C under wet and dry operation modes. For comparison, the cell employing the recast Nafion® membrane was operated at the same conditions.

2.2.8. Areal resistance measurement

EIS measurements were carried out to obtain the areal resistance of the membranes under wet and dry operation modes. A frequency response detector (EG&G Model 1025, Princeton Applied Institute) and a potentiostat/galvanostat (EG&G Model 273A, Princeton Applied Institute) were employed for the measurements. The areal resistances of the cells operating at the current density of 100 mA cm^{-2} under wet and dry conditions were measured.

3. Results and discussion

3.1. XRD analysis of the SiO_2–SZ particles

Fig. 2 showed the XRD patterns of SiO_2 and SiO_2–SZ particles after heating treatment. From this figure, it was observed that the SiO_2 particles were amorphous. However, this situation was different for SiO_2–SZ particles. The diffraction peak at $2\theta = 30.2°$ indicated that the tetragonal phase of SZ appeared in SiO_2–SZ particles. The patterns agreed with the results reported by Akkari et al. [36]. The results confirmed that the SZ was dispersed onto the surfaces of the SiO_2 support and the SiO_2 supported SZ particles could be prepared in the described experimental conditions.

3.2. FT-IR spectrum of the SiO_2–SZ particles

To gain some useful structure information of the SiO_2–SZ and SiO_2 particles, the FT-IR absorbance spectrum was conducted (Fig. 3). In the spectrum of SiO_2, it was observed an adsorption band at 1101 cm^{-1} corresponding to asymmetrical mode of Si–O bonds vibration in four-coordinated $SiO_2{}^{-4}$ species (Q_4) in oxide phase and on its surface. This band was typical for the pure amorphous silicon oxide. And the band of 960 cm^{-1} was attributed to Q_3 structures containing three-coordinated silicon. This process was typical for the formation of MCM-41-like structures [37].

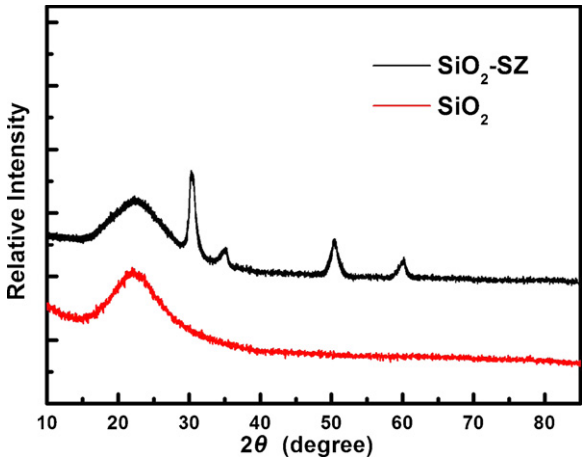

Fig. 2. XRD pattern of the SiO_2–SZ and SiO_2 particles. (For interpretation of the references to colour in the artwork, the reader is referred to the web version of the article.)

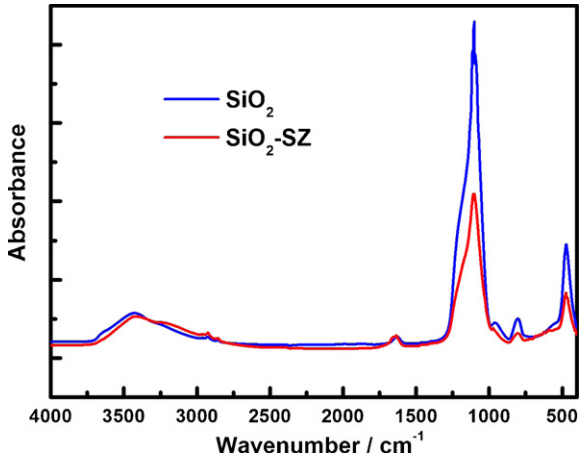

Fig. 3. FT-IR spectrum of the SiO_2–SZ and SiO_2 particles. (For interpretation of the references to colour in the artwork, the reader is referred to the web version of the article.)

In comparison with the IR spectrum of pure SiO_2, the maximum of the Si–O bands of SiO_2–SZ Q_4 structure vibrations in the oxide phase shifts to higher wave numbers of 1103 cm^{-1} and the band of SiO_2–SZ Q_3 structure vibrations almost disappears. This result indicated that the adding SZ decreased the vibrations of Si–O, and SZ interacted with SiO_2 at the molecular level. From the shifting peak and weaken strength of the vibration band, it might be deduced that a vibration of Zr–O–Si existed between SZ and SiO_2 [38].

3.3. SEM–EDS measurements of Nafion®/SiO_2–SZ composite membrane

To investigate the cross-sectional morphology of the Nafion®/SiO_2–SZ composite membrane and the distribution of the SiO_2–SZ particles in the polymer matrix, the SEM–EDS measurement was conducted and the image was shown in Fig. 4. It was obvious to see that the phenomenon of phase separation and particles congregation was not found. The result confirmed that the composite membrane was not only very dense and smooth, but the polymer and the inorganic particles also had good compatibility.

The EDS analysis of silicon and zirconium elements on the membrane cross-section can well characterize the distribution of SiO_2–SZ particles in the polymer matrix. From Fig. 4 (II), it was observed that the silicon, zirconium and sulfur elements distributed along the cross-section of the Nafion®/SiO_2–SZ composite membrane uniformly, which indicated a good distribution of SiO_2–SZ particles in the membrane. The uniform dispersion could increase the effective contact area between inorganic and organic phase and improve the interfacial compatibility. Especially, it was noticeable that the fluorine element aggregate domains were imaged close to the surface. Zawodzinski et al. [39] also found a fluorocarbon layer probably dominated the entire outermost several tenths of a nanometer of the surface.

3.4. IEC value and water uptakes measurement of the membranes

Table 1 listed the IEC values and the water uptakes of the three membranes namely the Nafion®/SiO_2–SZ, Nafion®/SiO_2 and recast Nafion®. The Nafion®/SiO_2–SZ membrane showed the highest IEC value of 0.93 mmol g^{-1} compared with the recast Nafion® of 0.90 mmol g^{-1} and the Nafion®/SiO_2 of 0.87 mmol g^{-1}. The increased IEC value illustrated that a little more acid sites resulting

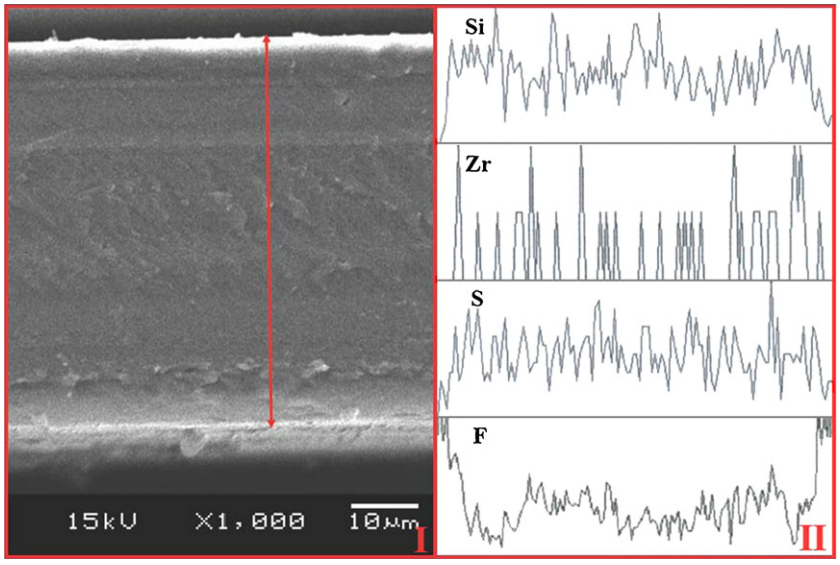

Fig. 4. SEM–EDS image of the Nafion®/SiO_2–SZ composite membrane.

Table 1
Comparison of IEC values and total/bulk/bound water content of the Nafion®/SiO_2–SZ, Nafion®/SiO_2 and recast Nafion® membranes

Membrane type	Thickness (μm)	IEC (mmol g^{-1})	Water uptake (%)			λ_{H_2O/SO_3H}		
			Total	Bulk	Bound	Total	Bulk	Bound
Nafion®/SiO_2–SZ	50	0.93	54.8	53.9	0.9	32.6	32.1	0.5
Nafion®/SiO_2	50	0.87	50.5	49.9	0.6	32.3	31.9	0.4
Recast Nafion®	50	0.90	30.2	29.8	0.4	18.5	18.3	0.2

from acidic SiO_2–SZ particles existed in Nafion®/SiO_2–SZ composite membrane. The enhanced acid property was expected to promote the membrane proton conductivity at various conditions [25–27]. On the contrary, Nafion®SiO_2 membrane showed the lowest IEC value due to the existence of non-proton-conductive SiO_2 particles. Obviously, this result was unfavorable to cell performance under wet condition.

Water uptake is an important property for PEMs which needs to be seriously considered, because the loss of water is anticipated to bring two negative impacts on cell performance: decreased proton conductivity and degraded membrane-catalyst interface [40–42]. To verify the improved hygroscopic property of membranes by incorporating SiO_2–SZ and SiO_2 particles, the water uptakes were measured. According to the Eikerling's theory, there are two kinds of water in PEMs [43]: one is bound water which solvates the sulfonic groups; the other is bulk water which fills the micro-pores. The total water and bound water can be respectively measured by weighting and TGA methods [33], and the bulk water is obtained by subtracting of the bound water from the total water.

To compare the bound water content of three membranes, the TGA measurement was applied [44]. In this method, the weight percentages of the three membranes at 100 °C were all held at 100% so as to simplify the comparison of water loss. As shown in Fig. 5, it could be seen that the Nafion®/SiO_2–SZ membrane showed the bound water content of 0.9 wt.% (in ΔW formation), which was higher than Nafion®/SiO_2 of 0.6 wt.% and recast Nafion® of 0.4 wt.%. The increased bound water content of composite membrane was attributed to the following two reasons: one was the incorporated SiO_2–SZ and SiO_2 particles in the composite membrane could contribute to better absorbing/retaining water properties than pristine Nafion® membrane. The other was SiO_2–SZ particles could supply more acid-like sites to absorb water compared with the Nafion®/SiO_2 and pristine Nafion® membranes. So the order of total bound water content (in ΔW formation) was Nafion®/SiO_2–SZ > Nafion®/SiO_2 > recast Nafion®. Although the total bound water content of two composite membranes was different, the bound water molecule of per $-SO_3H$ (in λ formation in Table 1) was very close and twice higher than that of recast Nafion®. It was shown that the SiO_2–SZ and SiO_2 had similar water absorbing property.

The total and bulk water content were shown in Table 1. From this table, the two composite membranes indicated almost twice higher water uptakes and λ_{H_2O/SO_3H} values than those of the recast Nafion® membrane. The increased water content in the composite membranes was due to highly hygroscopic property of SiO_2–SZ and SiO_2 particles, which in turn contributed to the good single cell performance under low RH condition [44]. This water absorbing property confirmed that the SiO_2–SZ particles retained the hygroscopic advantage of SiO_2.

3.5. Proton conductivity of the membranes

To measure the proton conductivity of the membranes, the EIS technique was employed. As shown in Fig. 6, the proton conductivity of Nafion®/SiO_2–SZ, Nafion®/SiO_2 and recast Nafion® under dry and wet H_2/O_2 conditions at 60 °C were compared. It was obvious that the two composite membranes showed higher proton conductivity in contrast to the pristine membrane under RH = 0% mode with the order Nafion®/SiO_2–SZ > Nafion®/SiO_2 > recast Nafion®. This was attributed to the hygroscopic property of SiO_2 and incorporative hygroscopic and acidic properties of SiO_2–SZ particles. Under RH = 100% mode, the Nafion®/SiO_2–SZ composite membrane also exhibited the highest proton conductivity values among the three membranes. For example, the proton conductivity of Nafion®SiO_2–SZ membrane was 6.95×10^{-2} S cm^{-1} and the value was higher than Nafion®/SiO_2 membrane of 5.54×10^{-2} S cm^{-1} and recast Nafion® membrane of 6.55×10^{-2} S cm^{-1}. The lower proton conductivity of Nafion®/SiO_2 membrane comparing with recast

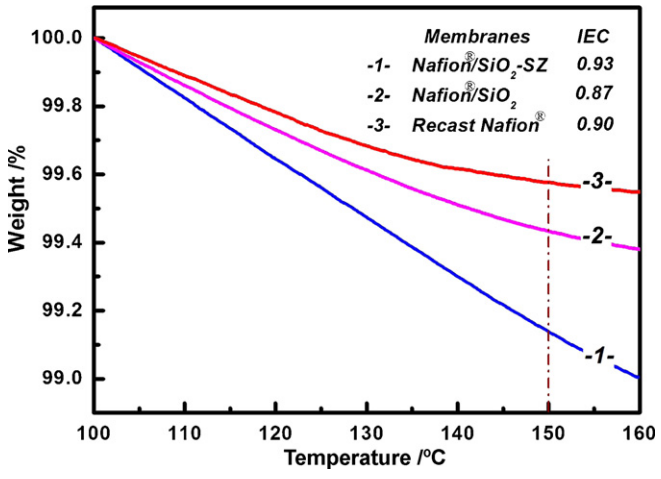

Fig. 5. The bound water content comparison of the Nafion®/SiO_2–SZ, Nafion®SiO_2 and recast Nafion® membranes measured by TGA.

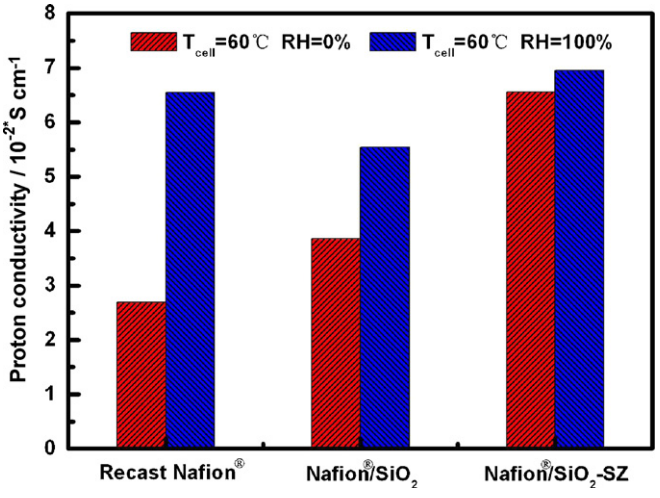

Fig. 6. Proton conductivity of the Nafion®/SiO_2–SZ, Nafion®/SiO_2 and recast Nafion® membranes at 60 °C under wet and dry conditions.

Nafion® under RH = 100% condition was due to the non-proton-conductive property of SiO_2.

In order to better understand some of the key factors involved in design of a composite membrane, some quantitative models of the conductivity are obtained. One of these models is based on the dusty-fluid model [41,45]. It is claimed that the proton diffusion obstruction presented in the polymer matrix is viewed as an additional frictional interaction with large immobile dust or gel particles. Within this framework, the inorganic additive is simply considered as an additional dust species immobilized within the polymer matrix. If the incorporated components are non-conductive (like SiO_2 particles), the proton diffusive resistance will be increased. So the objective of increased PEM conductivity can be achieved by the presence of acidic additives (like SiO_2–SZ particles) [41]. The presence of acid sites on the surface of SiO_2–SZ nanoparticles increases the total numbers of acid sites within the PEM, which correspondingly increases the available numbers of charge carriers and offers more effective proton transfer channels to enhance the proton conductivity (Fig. 1).

3.6. Single PEM fuel cell evaluation

Fig. 7 showed the single cell performances of Nafion®/SiO_2–SZ, Nafion®SiO_2 and recast Nafion® with wet H_2 and O_2 at T_{cell} = 60 °C, respectively. From Fig. 7, it was observed that the Nafion®/SiO_2 composite membrane exhibited the worst output performance (0.864 W cm^{-2}) due to the increased proton-conductive resistance caused by incorporated less proton-conductivity of SiO_2 particles. In contrast, Nafion®/SiO_2–SZ composite membrane showed similar cell performance to recast Nafion® (1.045 W cm^{-2} vs. 1.014 W cm^{-2}), because the incorporated SiO_2–SZ particles could effectively increase acid sites in polymer matrix and accordingly minimize the loss of proton conductivity. This result was well in consistent with previous proton conductivity measurement.

Fig. 8 indicated the single cell performance of these three membranes with dry H_2 and O_2 at T_{cell} = 60°C. In comparison with the recast Nafion® membrane (0.635 W cm^{-2}), the Nafion®/SiO_2–SZ (0.980 W cm^{-2}) and Nafion®/SiO_2 (0.742 W cm^{-2}) composite membranes showed better cell performance, which confirmed the poor proton conductivity of pristine Nafion® membrane under dry condition and manifested good water-retention property of Nafion®/SiO_2–SZ and Nafion®/SiO_2 composite membranes. It was noticeable that the performance of Nafion®/SiO_2–SZ membrane was superior to Nafion®/SiO_2 membrane. This was due to the SiO_2–SZ particles associated the hygroscopic property of SiO_2 with the proton conductivity of SZ, which could adsorb more water to enlarge the cluster size and supply extra channels to transfer proton. So the improvement result was Nafion®/SiO_2–SZ > Nafion®/SiO_2 > recast Nafion®.

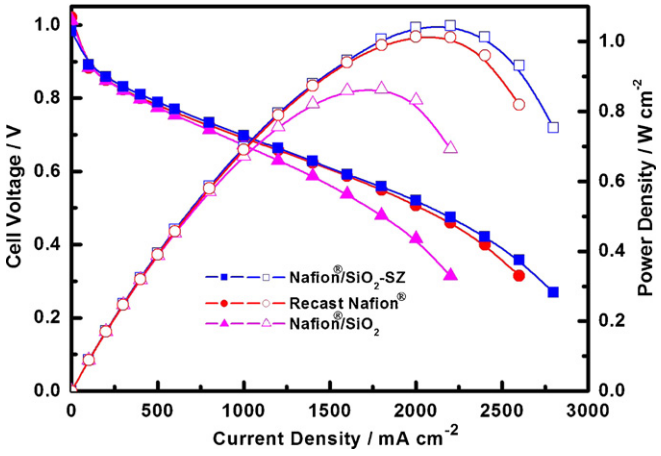

Fig. 7. Performance comparison of single cell employing the Nafion®/SiO_2–SZ, Nafion®/SiO_2 and recast Nafion® membranes with wet H_2/O_2 at 60 °C.

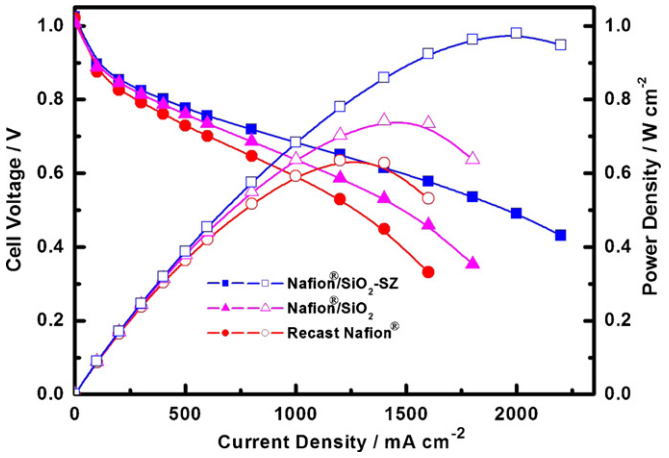

Fig. 8. Performance comparison of single cell employing the Nafion®/SiO_2–SZ, Nafion®/SiO_2 and recast Nafion® membranes with dry H_2/O_2 at 60 °C.

To further compare the self-humidifying effect of the two composite membranes, the peak power density fractions for the composite and recast Nafion® membranes were introduced. The values were calculated by comparing the peak power density values at dry and wet conditions. Table 2 listed the peak power density fractions for the Nafion®/SiO_2–SZ, Nafion®/SiO_2 and recast Nafion® membranes, respectively. From this table, it was shown that the fraction values of two composite membranes were higher than recast Nafion® membrane and the Nafion®/SiO_2–SZ membrane exhibited the highest. From this result, it could be deduced that the Nafion®/SiO_2–SZ composite membrane showed similar cell performance under wet and dry conditions, which indicated the cell performance of Nafion®SiO_2–SZ composite membrane was less dependent on RH change. The bi-functional SiO_2–SZ particles increased the proton conductivity capability and regulated the water balance in polymer matrix.

3.7. Areal resistance of the MEAs

To confirm the high single cell performance employing the Nafion®/SiO_2–SZ membrane, the EIS technique was used to measure the areal resistance of the three membranes under dry and wet conditions at 60 °C. From Table 3, the areal resistance values of Nafion®/SiO_2–SZ, Nafion®/SiO_2 and recast Nafion® membranes under dry condition at 100 mA cm^{-1} were 0.08, 0.12 and 0.30 Ω cm^2, respectively. The value of Nafion®/SiO_2–SZ membrane under dry condition was slightly higher than the value of recast Nafion® under wet condition (0.080 Ω cm^2 vs. 0.077 Ω cm^2). The lower areal resistance for the two self-humidifying membrane under dry condition was attributed to the incorporation of hygro-

Table 2
Comparison of the fraction of peak power density delivered by a PEMFC employing the Nafion®/SiO_2–SZ, Nafion®/SiO_2 and recast Nafion® membranes at 60 °C under wet and dry conditions

Membrane type	The peak power density (W cm^{-2})		Fraction of peak power density (%)
	RH = 0% mode	RH = 100% mode	
Nafion®/SiO_2–SZ	0.980	1.045	93.8
Nafion®/SiO_2	0.742	0.864	85.9
Recast Nafion®	0.635	1.014	62.6

Table 3
Comparison of areal resistance of the Nafion®/SiO_2–SZ, Nafion®/SiO_2 and recast Nafion® membranes at 60 °C under wet and dry conditions

Membrane type	Thickness (μm)	IEC (mmol g^{-1})	Areal resistance ($\Omega\,cm^2$)	
			RH = 0% mode	RH = 100% mode
Nafion®/SiO_2–SZ	50	0.93	0.080	0.073
Nafion®/SiO_2	50	0.87	0.12	0.091
Recast Nafion®	50	0.90	0.30	0.077

scopic SiO_2–SZ and SiO_2 particles. Compared to SiO_2 additive, the SiO_2–SZ particles had more contribution to decrease the areal resistance under dry operation due to its proton-conductive property.

4. Conclusions

In this paper, a novel Nafion®/SiO_2–SZ self-humidifying membrane was prepared by solution-casting method. The design of composite membrane was based on the consideration of improving the cell performance at low RH and minimizing proton conductive loss caused by incorporating hygroscopic SiO_2. The particles and its composite membrane were characterized by XRD, FT-IR, SEM and EDS techniques. The physical and chemical properties among Nafion®/SiO_2–SZ membrane, Nafion®SiO_2 membrane and recast Nafion® membrane were conducted. As a result, the Nafion®/SiO_2–SZ membrane exhibited highest IEC value, water uptakes, proton conductivity capacity, single cell performance and lowest areal resistance. The improved performance was due to the bi-functional effect of SiO_2–SZ particles which combined proton conductivity with water absorbing properties. The Nafion®SiO_2–SZ membrane showed a peak power density of 0.980 W cm^{-2} under dry H_2/O_2 condition at 60 °C compared with 0.742 W cm^{-2} of Nafion®/SiO_2 and 0.635 W cm^{-2} of recast Nafion®. Furthermore, the decreased areal resistance confirmed the proton-conductive and hygroscopic properties of SiO_2–SZ particles in composite membrane. As a promising candidate, Nafion®/SiO_2–SZ self-humidifying membrane could be applicable in PEMFCs under dry or low humidity operation.

Acknowledgement

This work was supported by National Natural Science Foundation of China (20476104).

References

[1] B.C.H. Steele, A. Heinzel, Nature 414 (2001) 345.
[2] S.M. Haile, D.A. Boysen, C.R.I. Chisholm, R.B. Merle, Nature 410 (2001) 910.
[3] S. Srinivasan, D.J. Manko, H. Koch, M.A. Enayetullah, A.J. Appleby, J. Power Sources 29 (1990) 367.
[4] U. Beuscher, S.J.C. Cleghorn, W.B. Johnson, Int. J. Energy Res. 29 (2005) 1103.
[5] M.K. Kadirov, A. Bosnjakovic, S. Schlick, J. Phys. Chem. B 109 (2005) 7664.
[6] T.A. Zawodzinski Jr., T.E. Springer, F. Uribe, S. Gottesfeld, Solid State Ionics 60 (1993) 199.
[7] R.S. Yeo, J. Electrochem. Soc. 130 (1983) 533.
[8] R. Hill, M.W. Verbrugge, J. Electrochem. Soc. 137 (1990) 886.
[9] D.M. Bernardi, J. Electrochem. Soc. 137 (1990) 3344.
[10] M. Cappadonia, J.W. Erning, S.M. Saberi Niaki, U. Stimming, Solid State Ionics 77 (1995) 65.
[11] T.A. Zawodzinski Jr., C. Derouin, S. Radzinski, R.J. Sherman, V.T. Smith, T.E. Springer, S. Gottesfeld, J. Electrochem. Soc. 140 (1993) 1041.
[12] T.F. Fuller, J. Newman, J. Electrochem. Soc. 139 (1992) 1332.
[13] P.L. Antonucci, A.S. Arico, P. Creti, E. Ramunni, V. Antonucci, Solid State Ionics 125 (1–4) (1999) 431.
[14] K.T. Adjemian, S. Srinivasan, J. Benziger, A.B. Bocarsly, J. Power Sources 109 (2002) 356.
[15] M. Watanabe, H. Uchida, Y. Seki, M. Emori, P. Stonehart, J. Electrochem. Soc. 143 (12) (1996) 3847.
[16] S.P. Nunes, B. Ruffmann, E. Rikowski, S. Vetter, K. Richau, J. Membr. Sci. 203 (2002) 215.
[17] V.S. Silva, B. Ruffmann, H. Silva, Y.A. Gallego, A. Mendes, L.M. Madeira, S.P. Nunes, J. Power Sources 140 (2005) 34.
[18] G. Zhang, Z. Zhou, J. Membr. Sci. 261 (2005) 107.
[19] A.S. Arico, V. Baglio, A.Di. Blasi, P. Creti, P.L. Antonucci, V. Antonucci, Solid State Ionics 161 (2003) 251.
[20] V. Baglio, A.S. Arico, A. Di Blasi, V. Antonucci, P.L. Antonucci, S. Licoccia, E. Traversa, F.S. Fiory, Electrochim. Acta 50 (2005) 1241.
[21] C.H. Rhee, H.K. Kim, H. Chang, J.S. Lee, Chem. Mater. 17 (2005) 1691.
[22] H. Munakata, H. Chiba, K. Kanamura, Solid State Ionics 176 (2005) 2445.
[23] Z.-G. Shao, P. Joghee, I. Hsing, J. Membr. Sci. 229 (2004) 43.
[24] G.D. Yadav, J.J. Nair, Micropor. Mesopor. Mater. 33 (1999) 1.
[25] Y. Zhai, H. Zhang, J. Hu, B. Yi, J. Membr. Sci. 280 (2006) 148.
[26] Y. Zhang, H. Zhang, Y. Zhai, X. Zhu, C. Bi, J. Power Sources 168 (2007) 323.
[27] Y. Zhang, H. Zhang, X. Zhu, C. Bi, J. Phys. Chem. B 111 (2007) 6391.
[28] Y. Sun, S. Ma, Y. Du, L. Yuan, S. Wang, J. Yang, F. Deng, F.-S. Xiao, J. Phys. Chem. B 109 (2005) 2567.
[29] J.R. Sohn, H.J. Jang, J. Mol. Catal. 64 (1991) 349.
[30] T. Lopez, J. Navarrete, R. Gomez, O. Novaro, F. Figueras, H. Armendariz, Appl. Catal. 125 (1995) 217.
[31] S. Damyanova, P. Grange, B. Delmon, J. Catal. 168 (1997) 421.
[32] S. Kaliaguine, S.D. Mikhailenko, K.P. Wang, P. Xing, G. Robertson, M. Guiver, Catal. Today 82 (2003) 213.
[33] B. Bahar, A.R. Hobson, J.A. Kolde, D. Zuckerbrod, U.S. Patent 5,547,551.
[34] Z.-G. Shao, H.-F. Xu, Solid State Ionics 177 (2006) 779.
[35] Y. Zhang, H. Zhang, X. Zhu, L. Gang, C. Bi, Y. Liang, J. Power Sources 165 (2007) 786.
[36] R. Akkari, A. Ghorbel, N. Essayem, F. Figueras, Micropor. Mesopor. Mater. 111 (2008) 62.
[37] S.M. Holmes, V.L. Zholobenko, A. Thursfield, R.J. Plaisted, C.S. Cundy, J. Dwyer, J. Chem. Soc., Faraday Trans. 94 (1998) 2025.
[38] H. Yang, R. Lu, L. Shen, L. Song, J. Zhao, Z. Wang, L. Wang, Mater. Lett. 57 (2003) 2572.
[39] T.A. Zawodzinski Jr., S. Gottesfeld, S. Shoichet, T.J. McCarthy, J. Appl. Electrochem. 23 (1993) 86.
[40] K.T. Adjemian, R. Dominey, L. Krishnan, H. Ota, P. Majsztrik, T. Zhang, J. Mann, B. Kirby, L. Gatto, M. Velo-Simpson, J. Leahy, S. Srinivasan, J.B. Benziger, A.B. Bocarsly, Chem. Mater. 18 (2006) 2238–2248.
[41] T.M. Thampan, N.H. Jalani, P. Choi, R. Datta, J. Electrochem. Soc. 152 (2) (2005) A316–A325.
[42] K. Kanamura, H. Morikawa, T. Umegaki, J. Electrochem. Soc. 150 (2003) A193.
[43] M. Eikerling, A.A. Kornyshev, U. Stimming, J. Phys. Chem. B 101 (1997) 10807.
[44] X. Zhu, H. Zhang, Y. Zhang, Y. Liang, X. Wang, B. Yi, J. Phys. Chem. B 110 (2006) 14240–14248.
[45] E.A. Mason, A.P. Malinauskas, Gas Transport in Porous Media: The Dusty Gas Model, Elsevier, Amsterdam, 1983, p. 142.